



Abstract—Accurate estimates of age, somatic growth, maturity, and natural mortality are essential for effective conservation of endangered species. This study resulted in updated growth data and the first direct assessments of length at maturity and age at maturity for the endangered smalltooth sawfish (*Pristis pectinata*). A Bayesian approach using the von Bertalanffy growth function was applied to combine vertebral band counts, mark-recapture data, and results from increment analysis to estimate somatic growth and to derive age at maturity and natural mortality rates. Smalltooth sawfish grow rapidly in their first 3 years, reaching 235 cm stretch total length (STL), 3.2 times their mean length at birth (73.7 cm STL), before growth slows. Asymptotic length was 446 cm STL for males and 484 cm STL for females, with a Brody growth coefficient of 0.178 year^{-1} for males and 0.170 year^{-1} for females. We directly estimated median age at maturity as 6.9 years for males and 7.9 years for females, similar to previous indirect assessments. Constant natural mortality was estimated to be between 0.151 and 0.278 on the basis of life history surrogates. The oldest individual examined in this study was a 30.1-year-old female, confirming that the species exceeds 30 years in the wild. These results are vital for refining population recovery models, and they underscore the need for ongoing monitoring and data collection to support long-term recovery efforts.

Manuscript submitted 10 April 2025.
Manuscript accepted 11 June 2025.
Fish. Bull. 123:190–206 (2025).
Online publication date: 30 June 2025.
doi: 10.7755/FB.123.3.5

The views and opinions expressed or implied in this article are those of the author (or authors) and do not necessarily reflect the position of the National Marine Fisheries Service, NOAA.

Age, growth, maturity, and natural mortality of the smalltooth sawfish (*Pristis pectinata*) in Florida waters

Andrea M. Kroetz (contact author)¹
Alyssa Mathers²
Zachary A. Siders³
Andrew K. Wooley⁴

Lukas B. Heath⁴
Dylan M. Yakich⁴
Rachel M. Scharer⁵
Gregg R. Poulakis⁴

Email address for contact author: andrea@havenworth.org

¹ Cooperative Institute for Marine and Atmospheric Studies
Rosenstiel School for Marine and Atmospheric Science
University of Miami
In affiliation with Southeast Fisheries Science Center
National Marine Fisheries Service, NOAA
3500 Delwood Beach Road
Panama City, Florida 32408
Present address of contact author:
Havenworth Coastal Conservation
10616 Giddens Place
Palmetto, Florida 34221

² A.I.S. Inc.
In support of Southeast Fisheries Science Center
National Marine Fisheries Service, NOAA
3500 Delwood Beach Road
Panama City, Florida 32408

³ Fisheries and Aquatic Sciences
School of Forest, Fisheries, and Geomatics Sciences
University of Florida
7922 NW 71st Street
Gainesville, Florida 32653

⁴ Charlotte Harbor Field Laboratory
Fish and Wildlife Research Institute
Florida Fish and Wildlife Conservation Commission
585 Prineville Street
Port Charlotte, Florida 33954

⁵ U.S. Army Corps of Engineers
701 San Marco Boulevard
Jacksonville, Florida 32207

Population dynamics and viability models are essential for understanding growth and mortality and can be used to determine recovery potential for endangered species (Beissinger and McCullough, 2002; Carlson and Simpfendorfer, 2015). Accurate age estimates are critical to parameterizing these models and are needed in efforts to promote recovery and support effective conservation and management actions. However, data are often limited for endangered species because small populations cannot sustain any mortality, even for scientific purposes, and therefore obtaining

sufficient sample sizes for analyses can be challenging (Heupel and Simpfendorfer, 2010; Smart et al., 2013).

Sawfish (family Pristidae) populations have declined globally, with all 5 extant species currently among the most endangered elasmobranchs (Dulvy et al., 2016; Harry et al., 2024). In the United States, the smalltooth sawfish (*Pristis pectinata*) was commonly found from Texas to North Carolina, but because of fisheries bycatch and habitat loss, the core population is currently restricted to waters of southern Florida (Brame et al., 2019). Because of this precipitous decline,

the species was listed as endangered under the U.S. Endangered Species Act in 2003 (Federal Register, 2003).

At the time of that listing, limited life history data were available on the smalltooth sawfish. Simpfendorfer et al. (2008) produced the first growth estimates using juvenile length–frequency and tag-recapture data, although the models were uncertain for individuals >220 cm stretch total length (STL). They estimated the von Bertalanffy growth parameters: asymptotic size (L_{∞}) at 600 cm STL, the Brody growth coefficient (k) at 0.140 year⁻¹, and the age at which length is zero (t_0) at -0.86 years. Scharer et al. (2012) refined these estimates with vertebral band counts, estimating L_{∞} at 448 cm STL, k at 0.219 year⁻¹, and t_0 at -0.81 years. Although these studies provided the first estimates of key age and growth parameters, each faced limitations, such as a bias toward the size class for small juveniles (Simpfendorfer et al., 2008), a low sample size (number of samples [n]=15; Scharer et al., 2012), and the inability to estimate length at maturity.

Reproductive and maturity data remain scarce, with no published studies providing direct estimates of length at maturity or detailed reproductive information. However, results from preliminary analyses indicate that males mature at 340 cm STL, on the basis of clasper calcification and testosterone levels, and that females mature at 370 cm STL, on the basis of estradiol levels (Brame et al., 2019). Using the vertebrae-derived growth model of Scharer et al. (2012) in a population viability analysis, Carlson and Simpfendorfer (2015) estimated that maturity occurs at ages between 7 and 11 years and that individuals of this species live to a maximum age of 30 years in the wild. The oldest individual in the study by Scharer et al. (2012) was 14 years old, although they suggested that the species likely lived longer. There are no direct estimates of natural mortality for the smalltooth sawfish in the wild, but Carlson and Simpfendorfer (2015) provided indirect estimates, which they converted to survivorship using multiple life history methods to account for various mortality mechanisms. Data from recent fishery-independent surveys indicate a maximum length of 500 cm STL (Brame et al., 2019), and the maximum known length is 553 cm STL (Bigelow and Schroeder, 1953).

Despite these advances, additional data and refined methods were used in this study to update and assess age, growth, maturity, and natural mortality estimates for the smalltooth sawfish. We aimed to address data gaps using a large sample of vertebrae collected from carcasses reported to the U.S. Sawfish Recovery Hotline over more than 20 years. Additionally, fishery-independent field surveys have been conducted for over 2 decades (2001–present) by members of the Smalltooth Sawfish Recovery Implementation Team across southwest Florida, and necropsies have contributed new data, including direct measurements of lengths at birth and assessments of maturity, body–length relationships over the entire length range, and mark-recapture information.

Materials and methods

Sample collection and processing

Vertebrae were collected during necropsies of smalltooth sawfish reported to the U.S. Sawfish Recovery Hotline (by phone, 1-844-4SAWFISH; email, sawfish@myfwc.com; or [website](#) form). For each sawfish, STL was measured, sex was determined if possible, and maturity was assessed following standard methods for elasmobranchs. For males, maturity was determined by using clasper calcification and the presence of well-developed testes and epididymides (Stehmann, 2002; Hamlett, 2005). For females, maturity was assessed by using the presence of well-developed ovaries with vitellogenic follicles and large, well-developed uteri or the presence of embryos in the uteri (Stehmann, 2002; Hamlett, 2005). This research was conducted under endangered species permit numbers 1475, 15802, 17787, 21043, 22078, and 25864.

Vertebrae were extracted from beneath the first dorsal fin and frozen at -20°C until centra were cleaned of tissue with diluted hydrogen peroxide. Centra were sagittally sectioned at a thickness of 0.5 mm, by using an IsoMet Low Speed Saw¹ (Buehler Ltd., Lake Bluff, IL), and were mounted on microscope slides with Cytoseal 60 (Thermo Fisher Scientific Inc., Waltham, MA). Each section was observed under transmitted light with a stereo microscope (RZ series, Meiji Techno Co. Ltd., Saitama, Japan) at 7.5–50× magnification and photographed by using an image analysis system (Infinity 2, Teledyne Lumenera, Richmond, Canada).

Fishery-independent field research on this species has been ongoing since 2001, providing key information on length at birth, length relationships, and mark-recapture information, all of which was used in our modeling. At the time of this study, morphological data on 1600 live individuals had been collected, including sex, straight length measurements, and maturity assessments. Maturity for males was determined by using clasper calcification, and maturity for females was determined by using length-based estimates from Brame et al. (2019). Length data included 1) total rostral length (TRL), defined as the straight length of the rostrum from its tip to the midpoint, where the rostrum begins to flare at the confluence of the rostrum and head, 2) body length (BL), defined as the straight length from the base of the rostrum, where it begins to flare, to the tip of the maximally stretched caudal fin, and 3) STL, defined as the straight length from the tip of the rostrum to the tip of the maximally stretched caudal fin. Sawfish recaptured during surveys were designated as *mark-recapture* individuals, and measurements were taken at recapture to determine growth. Length at birth was derived from the survey data, with individuals considered neonates if remnants of a rostral sheath were

¹ Mention of trade names or commercial companies is for identification purposes only and does not imply endorsement by the National Marine Fisheries Service, NOAA, or the Florida Fish and Wildlife Conservation Commission.

present or the yolk-sac scar was open at time of capture (Poulakis et al., 2024).

Age assessment

Growth bands were identified as bright opaque bands that occurred in the corpus calcareum (edge) on one side of the vertebral section and extended through the intermedialia (middle) and back through the corpus calcareum on the other side of the section. Any bands that did not meet these criteria were not included in final band counts. The first opaque band was assumed to be the natal mark (Tanaka, 1991; Cailliet and Goldman, 2004). Subsequent opaque bands were interpreted as annual marks, as annual band formation has been verified for this species (Scharer et al., 2012). Opaque bands visible on the outer margin were included in the final counts. Two independent readers read each slide twice without prior knowledge of STL or sex to ensure that there was no bias. Age readings were compared, and if there was disagreement, both readers read the slides again and reached a consensus. Within-reader precision was computed with reader counts by using average percent error following Beamish and Fournier (1981). Estimated total days alive (i.e., fractional age) was calculated by subtracting a standardized birth date (i.e., 15 April; Poulakis et al., 2011; Scharer et al., 2012) from the capture date, and dividing by 365.

Data analysis

Formulation of a von Bertalanffy growth function We fit a Bayesian implementation of the von Bertalanffy growth function (VBGF) (von Bertalanffy, 1938). We used a multiple likelihood approach to incorporate 3 different growth information sources—vertebral band counts, mark-recapture data, and results from increment analysis. We ran 4 versions of the VBGF split by the data types: 1) the full combined model, 2) a version using only vertebral band counts, 3) a version using only mark-recapture data, and 4) a version using only results from increment analysis. This use of different versions allowed us to assess the contribution of each type of growth data to the overall model.

For increment analysis, photographs were taken of each vertebral section, and using these images, we measured the distance from the center of the vertebrae to the center of each growth band in ImageJ, vers. 1.54g (Schneider et al., 2012). We then rescaled the optical distances (pixels) to be between 0 and 1 using this equation to generate the relative increment distance ($\varphi_{i,t}$):

$$\varphi_{it} = \frac{d_{i,t} - \min(d_i)}{\max(d_i) - \min(d_i)}, \quad (1)$$

where $d_{i,t}$ = the optical increment distance from the center of the vertebrae at a given band and time t for individual i .

These relative increment distances were used in the VBGF estimation.

Across models, we used a data-informed length at birth following Rolim et al. (2020), Caltabellotta et al. (2021), and Siders et al. (2023):

$$L_{0,i} \sim \text{lognormal}\left(\log\left(\hat{L}_0\right), \sigma_{L_0}\right), \quad (2)$$

where $L_{0,i}$ = the observed length-at-birth information from neonate i ;

\hat{L}_0 = the estimated mean length at birth; and

σ_{L_0} = the standard deviation in the length at birth.

For vertebral band counts and increment analysis, we used the length-at-birth formulation of the VBGF:

$$\hat{L}_{i,t} = L_{\infty} - (L_{\infty} - L_0)e^{-kt_i}, \text{ and} \quad (3)$$

$$L_i \sim \text{lognormal}\left(\hat{L}_{i,t}, \sigma_X\right), \quad (4)$$

where $\hat{L}_{i,t}$ = the STL at some predicted time (age) t of individual i ;

t_i = time (age) of individual i ;

L_i = the observed length of individual i ; and

σ_X = the lognormal growth variability that matches the observation process, where X is either vertebral counts (σ_{VC}) or increment analysis (σ_{IA}).

We further modified the length-at-birth model to account for sex-specific growth, while including individuals without an assigned sex, allowing L_{∞} , k , and σ_{VC} to receive additive effects of sex (Equations 5–7) to generate Equations 8 and 9 following Siders et al. (2023) and Chamberlin et al. (2025).

$$\log(L_{\infty,s}) = \log(L_{\infty}) + \beta_{L_{\infty},s}, \quad (5)$$

$$\log(k_s) = \log(k) + \beta_{k,s}, \quad (6)$$

$$\log(\sigma_{VC,s}) = \log(\sigma_{VC}) + \beta_{\sigma_{VC},s}, \quad (7)$$

$$\hat{L}_{i,t} = L_{\infty,s} - (L_{\infty,s} - L_0)e^{-k_s t_i}, \text{ and} \quad (8)$$

$$L_i \sim \text{lognormal}\left(\hat{L}_{i,t}, \sigma_{VC,s}\right), \quad (9)$$

where $\beta_{X,s}$ = the sex-specific additive effect to a given VBGF parameter X , and

θ_s = the sex-specific parameter.

Because we made the sex-specific effects additive, we could use Equation 3 to describe the von Bertalanffy growth curve for individuals without an assigned sex and Equation 8 to describe the growth for individuals with an assigned sex.

Some individuals with vertebral band counts did not have an observed STL. For those individuals, length-based relationships derived from survey data were used to

estimate the STL. We used 2 length-based relationships: 1) STL as a function of BL and 2) STL as a function of TRL:

$$L_i \sim \text{Normal}(\beta_{\text{BL},0} + \beta_{\text{BL},1} \times \text{BL}_i, \sigma_{\text{BL}}), \text{ and} \quad (10)$$

$$L_i \sim \text{Normal}(\beta_{\text{TRL},0} + \beta_{\text{TRL},1} \times \text{TRL}_i, \sigma_{\text{TRL}}), \quad (11)$$

where $\beta_{\text{BL},0}$ and $\beta_{\text{TRL},0}$ = the intercept;
 $\beta_{\text{BL},1}$ and $\beta_{\text{TRL},1}$ = the slope; and
 σ_{BL} and σ_{TRL} = the standard deviation.

Because these relationships generate their own source of error into the dependent variable of L_i , we chose to estimate these relationships simultaneously with the VBGF and to propagate the error forward. We then used these length-based relationships to predict the L_i of individuals without an STL, turning L_i into a latent random variable, L_i . This L_i was then used in either Equation 4 or 9, depending on whether the individual had an assigned sex. We prioritized BLs over TRLs when available.

We also accounted for the individual repeated measurements of the increment analysis by including individual random effects for L_∞ and k following Siders et al. (2023) and Suriyamongkol et al. (2024), with the mean of the individual random effects set at zero for each transformed growth parameter:

$$\begin{Bmatrix} \beta_{L_\infty,i} \\ \beta_{k,i} \end{Bmatrix} \sim \text{MVN} \left(\begin{Bmatrix} 0 \\ 0 \end{Bmatrix}, \Sigma \right), \quad (12)$$

where Σ = the covariance matrix of the multivariate normal distribution (MVN).

To ease the fitting of this correlation, we decomposed the covariance matrix with the Cholesky factorization (see Siders et al., 2023), effectively modifying Equations 5 and 6 to incorporate the additive individual random effect as follows:

$$\log(L_{\infty,i,s}) = \log(L_\infty) + \beta_{L_\infty,s} + \beta_{L_\infty,i}, \text{ and} \quad (13)$$

$$\log(k_{i,s}) = \log(k) + \beta_{k,s} + \beta_{k,i}. \quad (14)$$

Given that we allowed individual variation in the growth rate (informed by L_∞ and k), we did not estimate sex-specific effects on σ_{IA} .

Additionally, in the length-at-birth model, we conducted the back-calculation of length at time from the increment analysis within the model following Caltabellotta et al. (2021). In this back-calculation, the length at time was treated as a latent random variable, $L_{i,t}$, similar to how the length-based imputation was done, but it was informed by the length at capture, $L_{i,c}$, and the estimated length at birth:

$$L_{i,t} = \phi_{i,t} (L_{i,c} - L_0) + L_0, \quad (15)$$

where $\phi_{i,t}$ = the increment measurement at a specific vertebral band associated with age t , for individual

i , and relativized to the increment measurement at the maximum age (Equation 1).

By doing the back-calculation within the model, any uncertainty in the estimated length at birth was incorporated into back-calculated lengths at ages and propagated forward into uncertainty in L_∞ , k , σ_{IA} , and Σ .

We incorporated recaptured individuals using the Fabens (1965) mark-recapture version of the VBGF. We modified Equations 3 and 8 to be based on the $L_{i,c}$ and the time at large, Δt_i :

$$\hat{L}_{i,t} = L_\infty - (L_\infty - L_{i,c})e^{-k\Delta t_i} \text{ or } L_{\infty,s} - (L_{\infty,s} - L_{i,c})e^{-k_s\Delta t_i}, \text{ and} \quad (16)$$

$$L_i \sim \text{lognormal} \left(\hat{L}_{i,t}, \sigma_{\text{MR}} \right), \quad (17)$$

where σ_{MR} = the mark-recapture growth variability shared between sexes.

Typically, accounting for individual growth variability is necessary in the Fabens (1965) model (e.g., Taylor et al., 2005; Siders et al., 2023). However, given the augmentative nature of the mark-recapture data to the VBGF, we chose not to estimate individual random effects.

Model implementation We used the software Stan (vers. 2.36; Stan Development Team, 2024) with the package cmdstanr (vers. 0.8.1; Gabry et al., 2024) in R (vers. 4.4.1; R Core Team, 2024) to implement the Bayesian VBGF. We first fit Equation 3 using maximum-likelihood estimation to generate weakly informative priors, following Caltabellotta et al. (2019), Rolim et al. (2020), and Chamberlin et al. (2023), for L_∞ , k , and σ_{VB} and using the predicted mean for the prior location and a 30% coefficient of variation to generate the corresponding scale (Table 1). For L_∞ , k , σ_{VC} , σ_{MR} , and σ_{IA} , we specified normal priors on the log-transformed parameters. For \hat{L}_0 , we used the mean STL of the neonates on the log scale to set a normal prior, and for σ_{L_0} , we used a Cauchy distribution with a location of 0 and scale of 1. We specified normal priors with a mean of 0 and a standard deviation of 1 for the sex-specific additive effects as they were on the log- or logit-transformed scale following Chamberlin et al. (2025). Standard normal priors were put on β_0 and β_1 for the length-based relationships, and a Cauchy prior with location of 0 and scale of 2.5 were put on the corresponding σ . We set a prior on Σ following the Cholesky decomposition used in Siders et al. (2023).

Across models, we up-weighted the length-at-birth likelihood 10 times relative to the growth likelihoods to counteract the low sample size of the length-at-birth dataset. Lastly, for the combined model, we weighted the likelihoods by dividing the sample size of a given growth dataset by the total sample size across growth datasets and subtracting the result from 1. For each model, we used the no U-turn sampler in Stan with 8 chains that had 5000 warmup iterations and 125 sampling iterations each and a maximum tree depth of 15. We combined the chain-specific posterior samples to generate a single posterior

Table 1

Prior distributions used for parameters in the von Bertalanffy growth function (VBGF) fit to a combination of 3 data sources, vertebral band counts (VCs), mark-recapture (MR) data, and results from increment analysis (IA), for smalltooth sawfish (*Pristis pectinata*) in Florida. In other models, each of which were fitted to a single source, the same prior distribution for the subset of parameters relevant to each model was used. The VBGF parameters include the estimated mean length at birth (\hat{L}_0) and its standard deviation (σ_{L_0}), asymptotic length (L_∞), Brody growth coefficient (k), growth variability that matches a dataset (e.g., vertebral band counts [σ_{VC}]), and sex-specific additive effect to a given VBGF parameter (e.g., $L_\infty [\beta_{L_\infty,s}]$). For the relationships of stretch total length to body length (BL) and total rostral length (TRL), parameters include the intercept ($\beta_{BL,0}$ and $\beta_{TRL,0}$), slope ($\beta_{BL,1}$ and $\beta_{TRL,1}$), and standard deviation (σ_{BL} and σ_{TRL}). Parameters related to individual random effects on L_∞ and k of individuals with IA performed and with MR growth data include the Cholesky decomposition (L_X) of the covariance matrix (Ω_X), the variance of the random effects (τ_X), the nuisance parameter (γ_X) for transforming the variance prior distribution, and the mean random effect for L_∞ ($\beta_{L_\infty,i}$) and k ($\beta_{k,i}$).

	Parameter	Prior
VBGF	$\log\left(\hat{L}_0\right)$	$N(4.30,1.29)$
	σ_{L_0}	Cauchy(0,1)
	$\log(L_\infty)$	$N(6.12,1.84)$
	$\log(k)$	$N(-1.70,0.51)$
	$\log(\sigma_{VC}), \log(\sigma_{IA}),$ $\log(\sigma_{MR})$	$N(-1.84,0.55)$
	$\beta_{L_\infty,s}$	$N(0,1)$
	$\beta_{k,s}$	$N(0,1)$
	$\beta_{\sigma_{VC},s}$	$N(0,1)$
Length-length relationship	$\beta_{TRL,1}$	$N(0,1)$
	$\beta_{TRL,0}$	$N(0,1)$
	σ_{TRL}	Cauchy(0,2.5)
	$\beta_{BL,1}$	$N(0,1)$
	$\beta_{BL,0}$	$N(0,1)$
	σ_{BL}	Cauchy(0,2.5)
Random effects	$\Omega_{IA} = L_{\Omega_{IA}} \hat{L}'_{\Omega_{IA}}$	$L_{\Sigma_{IA}} \sim \text{LKJCholesky}(2)$
	$\Sigma_{IA} = \tau_{IA} \Omega_{IA} \tau_{IA}$	
	$\Omega'_{MR} = L_{\Omega_{MR}} \hat{L}'_{\Omega_{MR}}$	$L_{\Sigma_{MR}} \sim \text{LKJCholesky}(2)$
	$\Sigma_{MR} = \tau_{MR} \Omega_{MR} \tau_{MR}$	
	$\tau_{IA} = 2.5 \times \tan(\gamma_{IA})$	$\gamma_{IA} \sim U\left(0, \frac{\pi}{2}\right)$
	$\tau_{MR} = 2.5 \times \tan(\gamma_{MR})$	$\gamma_{MR} \sim U\left(0, \frac{\pi}{2}\right)$
	$\beta_{L_\infty,i}$	$N(0,1)$
	$\beta_{k,i}$	$N(0,1)$

of each parameter after assessing chain coverage with the Gelman and Rubin (1992) statistic set below 1.1 for all parameters. We assessed significant differences between parameters using the maximum a posteriori value at a significance level of 0.10 in the R package bayestestR (vers. 0.15; Makowski et al., 2019).

Predicted maturity and length-based growth Within the Bayesian VBGF, we derived age at maturity ($t_{IM,mat}$) using the reported length at maturity ($L_{IM,mat}$) from Brame et al. (2019) of 340 cm STL for males and 370 cm STL for females with a mean of 355 cm STL for pooled sexes:

$$t_{IM,mat} = \frac{1}{k} \log\left(\frac{L_\infty - L_0}{L_\infty - L_{IM,mat}}\right). \tag{18}$$

We predicted age at length from the VBGF over a range of hypothetical ages from zero to the maximum observed age by 0.1-year increments to estimate growth throughout the lifespan. This approach allowed us to calculate both age at capture and age at recapture for the recaptured individuals by adding the years spent at large between capture and recapture to the estimated age at capture.

We compared the back-calculated age at maturity based on indirect observations of maturity from Brame et al. (2019) with direct maturity estimates based on the observed developmental state of reproductive organs of necropsied individuals. We calculated the average length at 50% maturity, defined as the length at which 50% of the population reaches maturity, and the average age at 50% maturity, defined as the age at which 50% of the population reaches maturity, using a binomial logistic regression with probit link function. To estimate the means and 95% confidence intervals (95% CIs), we applied a bootstrap with replacement technique over 1000 iterations. Given that mature females tended to be larger than males in both length and weight, sexes were analyzed independently.

Predicted natural mortality and mortality at age We estimated constant natural mortality and natural mortality at age using the samples with known ages to generate a value of maximum observed age from the VBGF parameters. In the absence of direct estimates of natural mortality for sawfish, we used established mortality estimators derived from life history surrogates. To estimate constant natural mortality, we used the estimators from Pauly (1980), Hoenig (1983), and Jensen (1996), and, for natural mortality at age, we used the estimators from Peterson and Wroblewski (1984), Chen and Watanabe (1989), and Lorenzen (1996). The Peterson and Wroblewski (1984) and Lorenzen (1996) estimators used weight at age, which we generated from the posterior length-at-age predictions with the equation $W_t = 0.0004L_t^{2.56}$, following Simpfendorfer (2000) (Table 2). We also incorporated the maximum observed age and VBGF estimators for constant natural mortality from Then et al. (2015) and the best-fit model for natural mortality at age from Lorenzen et al. (2022) (see table 3 in Lorenzen et al., 2022; Table 2).

Table 2

Methods for estimation of constant natural mortality (M) or natural mortality at age (M_t). These surrogate estimators were used to derive estimates of natural mortality for the smalltooth sawfish (*Pristis pectinata*) from either the maximum observed age (t_{\max}) or parameters of the von Bertalanffy growth function, asymptotic length (L_{∞}), Brody growth coefficient (k), and age at which length is zero (t_0). Z =total instantaneous fishing mortality; T =temperature; W_t =weight at age; and L_t =length at age.

Method	Relationship
Hoenig (1983)	$\log(Z) = 1.46 - 1.01 \log(t_{\max})$
Pauly (1980) ¹	$\log(M) = -0.0066 - 0.279 \log(L_{\infty}) + 0.65543 \log(k) + 0.4634 \log(T)$
Jensen (1996)	$M = 1.6k$
Then et al. (2015)	$M = 4.899t_{\max}^{-0.916}$
Then et al. (2015)	$M = 4.118k^{0.73}L_{\infty}^{-0.33}$
Chen and Watanabe (1989)	$M_t = \frac{k}{1 + e^{-k(t-t_0)}}$
Peterson and Wroblewski (1984) ²	$M_t = 1.92W_t^{-0.25}$
Lorenzen (1996) ²	$M_t = 3.69W_t^{-0.305}$
Lorenzen et al. (2022)	$M_t = 0.28 - 1.3 \log\left(\frac{L_t}{L_{\infty}}\right) + 1.08 \log(k)$

¹ Consistent with Carlson and Simpfendorfer (2015), $T=22^{\circ}\text{C}$

² Consistent with Simpfendorfer (2000), $W_t = 0.0004L_t^{2.56}$

Results

From 2003 through 2024, vertebrae from 115 smalltooth sawfish were collected in Florida and used for age analysis. These fish included 47 males, 62 females, and 6 individuals that could not be assigned a sex because of decomposition. Among the males, 15 fish (31.9%) were mature, and 32 individuals (68.1%) were immature. Among the females, 19 fish (30.6%) were mature, 40 individuals (64.5%) were immature, and 3 individuals (4.8%) were too decomposed for maturity to be assessed. Smalltooth sawfish ranged from 60 to 490 cm STL, with males measuring 60–423 cm STL (mean: 259.7 cm STL) and females measuring 70–490 cm STL (mean: 280.4 cm STL) with a mean for pooled sexes of 266.9 cm STL (Fig. 1). For 101 of the 115 samples, a measurement of STL was available; length-based conversions were applied for the remaining samples.

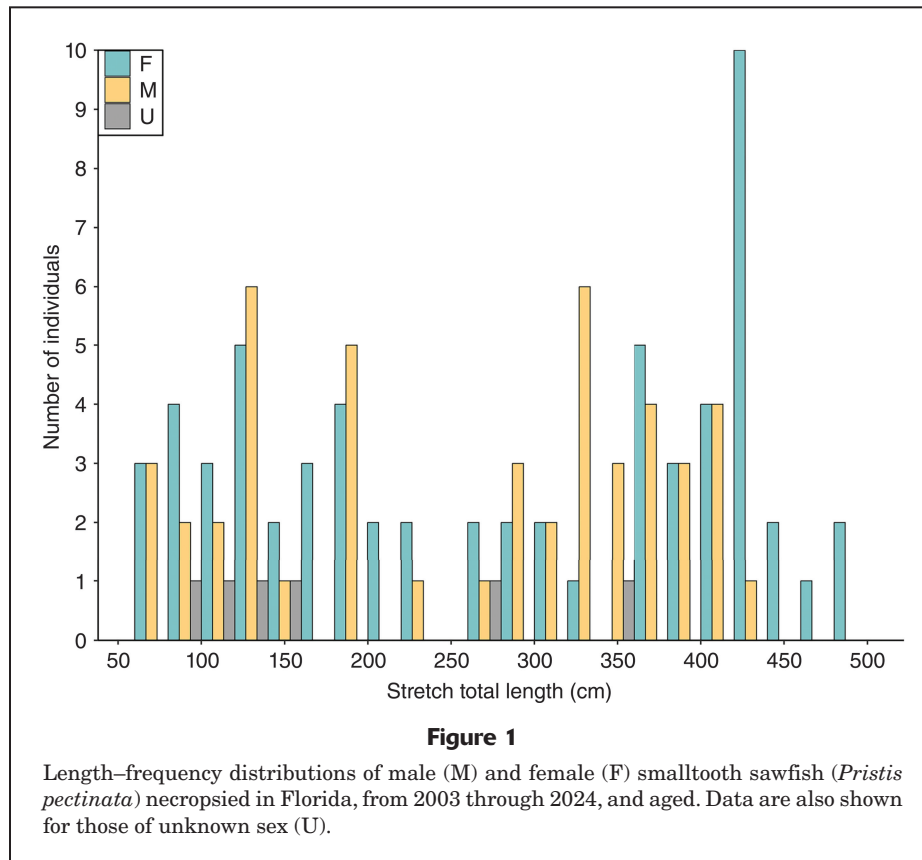
Length and age assessment

Length-based measurements from 1600 live sawfish were collected for over 20 years (2001–2023) during fishery-independent surveys, including from 744 males (693 immature and 51 mature), 853 females (817 immature and 36 mature), and 3 individuals of unknown sex. Stretch total lengths ranged from 58.1 to 488.2 cm, TRLs ranged from 15 to 110 cm, and BLs ranged from 43.0 to 386.2 cm. Contributing to the mark-recapture information, 174

fish were recaptured and measured, with 200 recapture events and a median of 1 recapture per individual ($n=152$), although some individuals were recaptured 2 ($n=18$) or 3 ($n=4$) times. Time at liberty between recapture events ranged from the same day to 10.8 years, with a median of 0.2 years and mean of 0.7 years. The individual with the longest time at liberty was an immature male that was captured in 2003 at 78.5 cm STL and recovered dead in 2024, 10.8 years later, mature, at an STL of 407.8 cm.

Opaque bands on vertebrae were apparent and discernible with bands becoming more tightly spaced and diffuse with age (Fig. 2). A 75.7% agreement was reached between readers with an average coefficient of variation of 6.1 and an average percent error of 4.3%. For 72.4% of the individuals ($n=20$) for which readers had different age estimates, the disagreement was attributed to a difference in 1 band count. The fractional age of the youngest individual for both males and females was 0.0 years. The oldest female was 30.1 years old, and the oldest male was 22.1 years old (Fig. 3). Notably, 45.2% of samples were <3 years old, 43.5% were between 4 and 12 years old, 6.1% were between 13 and 19 years old, and 5.2% were >20 years old.

Increment analysis was performed for 39 individuals, resulting in 424 increments that were used in the VBGFs. These individuals ranged in age from 6 to 29 years (median: 11.0 years) and in length from 314.2 to 490.0 cm STL (mean: 386.1 cm STL).



Model comparison

Convergence was reached in all 4 models, with the Gelman and Rubin (1992) statistic below 1.1 for all parameters. Among models, the combined model was the most certain in its posterior estimates of VBGF parameters, outperforming the model fit to only vertebral band counts (2.0–2.3 times for L_{∞} and 2.5–3.0 times for k), the model fit to only mark-recapture data (2.4–3.3 times for L_{∞} and 2.7–3.6 times for k), and the model fit to results from increment analysis (1.7–1.8 times for L_{∞} and 1.1–1.3 times for k). Even with information on length at birth provided to each VBGF, the uncertainty of the vertebral-band-count model and the mark-recapture model was 3.2 and 3.3 times greater than that of the combined model in the posterior parameter estimates of length at birth. There was no difference in uncertainty between the combined model and the vertebral-band-count model in the length-based relationships. However, the length-based relationship of STL to BL ($STL=3.49+1.27BL$) had less variability (median σ_{BL} : 0.0146 cm) than the relationship of STL to TRL ($STL=-8.8+4.57TRL$) (median σ_{TRL} : 0.0526 cm) across all models (Table 3; Fig. 3, A and B). As a result, the estimated STL for aged individuals without an observed STL was more uncertain for the 3 individuals for which predictions were made by using the STL–TRL relationship (Fig. 3C).

The best estimates were produced with the combined model. Smalltooth sawfish grew rapidly during their first 3 years, reaching approximately 235 cm STL, 3.2 times their length at birth (Fig. 3). The maximum a posteriori estimate indicates that smalltooth sawfish are born at 73.7 cm STL (lognormal standard deviation of 0.07). Estimates of L_{∞} are 446 cm STL for males, 484 cm STL for females, and 464 cm STL for pooled sexes (Table 3, Fig. 3). The k estimates are 0.178 year⁻¹ for males, 0.170 year⁻¹ for females, and 0.174 year⁻¹ for pooled sexes. Standard deviations for lognormal vertebral count growth (males: 0.163; females: 0.188; pooled: 0.175) are greater than those for lognormal growth based on mark-recapture data (pooled: 0.0635) and growth based on increment analysis (pooled: 0.0519). The lower variability in growth estimates is reflected in the tighter clustering of small individuals in the mark-recapture dataset (Fig. 4) and the increment analysis dataset (Fig. 5) compared to that in the vertebral-band-count dataset (Fig. 3C). Among the growth parameters, only L_{∞} significantly differs between sexes ($P=0.072$) (Table 4).

Estimates of growth model parameters vary across models because of differences in length distributions among individuals that were aged, recaptured, and used in increment analysis (Table 3). The mark-recapture model was heavily influenced by the lack of large individuals (>300 cm STL), resulting in the lowest estimates of L_{∞} ,

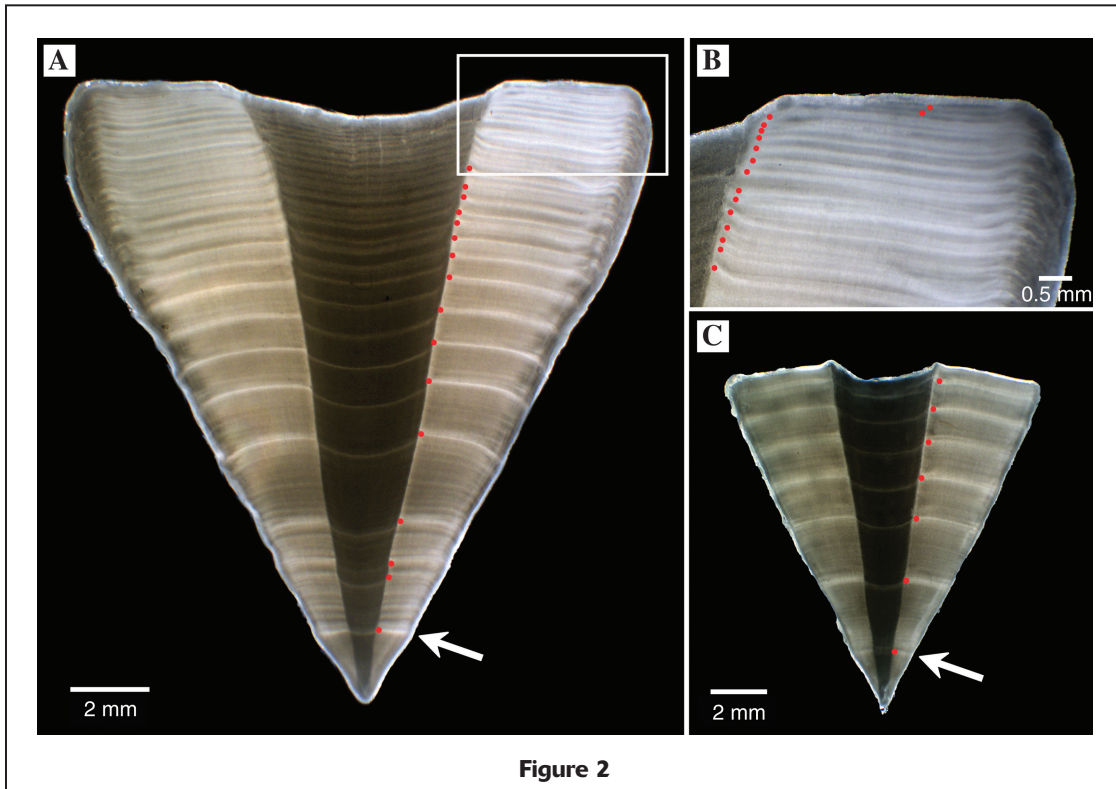


Figure 2

Vertebral sections from smalltooth sawfish (*Pristis pectinata*) necropsied in Florida in 2021. Red dots indicate annual growth bands, and the white arrow in each section indicates the first band (closest to the center of the vertebra), which is the natal mark. (A) This large section is from the oldest and second-longest animal in the study, a female with a stretch total length of 488.2 cm and an estimated age of 30.1 years. (B) A close-up view, this image shows how bands became stacked in the oldest individuals (the area in this image is indicated in panel A by the box outlined in white). (C) This section is from a vertebra typical of those aged in this study; it is from a female with a stretch total length of 376.5 cm and estimated age of 6.0 years.

approximately 90%–93% of the estimates from the combined model. Minimal growth between capture events for 2 individuals, growth of $0.04 \text{ cm year}^{-1}$ for their 7.1 and 0.5 years at large, heavily influenced L_{∞} (Fig. 4). Similarly, the increment analysis model had few large individuals, leading to 1.7–1.8 times more uncertainty in L_{∞} estimates than the combined model and increased posterior estimates of k (Table 3, Fig. 5). The vertebral-band-count model generally had smaller L_{∞} estimates and higher k estimates than the combined model, and the uncertainty of this model in these parameter estimates is greater than that of the combined model (Table 3).

In comparisons between model estimates of age at length and estimates of age at recapture based on years at large from recapture events, recapture events fall into 3 groups. For about one-third of the 200 recapture events (74 events), estimates are not significantly different. In contrast, age-at-recapture estimates based on data from the remaining 126 recapture events are significantly different from model predictions: age at recapture for 33% (66 events) is lower and for 30% (60 events) is higher than the model estimate. Median differences, however, are small (-0.1 years and 0.1 years, respectively), indicating that model estimates are generally accurate.

Maturity

The indirect estimates from Brame et al. (2019) used in the VBGF indicate that length at maturity occurred at 76.3% of L_{∞} (340.3 cm STL; 90% credible interval: 72.7%–80.0%) for males and at 76.5% of L_{∞} (370.3 cm STL; 90% credible interval: 73.4%–79.4%), for females (Table 3). The coinciding maximum a posteriori age at maturity for these lengths at maturity were 7.1 years for males and 7.6 years for females, with no significant difference in age at maturity between sexes ($P=0.42$, from the combined model) (Table 4). On the basis of direct estimates of maturity from examination of reproductive organs of necropsied individuals, males reached 50% maturity at 345.4 cm STL (95% CI: 334.9–355.0 cm STL; 77% of L_{∞}). The largest immature male was 346 cm STL (5.0 years old), and the smallest mature male was 345 cm STL (7.9 years old). For females, length at 50% maturity was estimated at 383.1 cm STL (95% CI: 371.4–397.2 cm; 79% of L_{∞}). The largest immature female was 390 cm STL (6.1 years old), and the smallest mature female was 378 cm STL (9.9 years old). For males, the resulting age at 50% maturity was estimated at 6.9 years (95% CI: 6.0–7.9 years). The oldest immature male was 7.0 years (365 cm STL), and the youngest

Table 3

Median estimates and 90% credible intervals (in parentheses) for the following parameters of 4 versions of the von Bertalanffy growth function used to examine age and growth of the smalltooth sawfish (*Pristis pectinata*): asymptotic length (L_∞); Brody growth coefficient (k); length at birth (L_0); variability in length at birth (σ_{L_0}); variability in length at age based on vertebral band counts (σ_{VC}), mark-recapture data (σ_{MR}), and results from increment analysis (σ_{IA}); intercept ($\beta_{BL,0}$ and $\beta_{TRL,0}$), slope ($\beta_{BL,1}$ and $\beta_{TRL,1}$), and variability (σ_{BL} and σ_{TRL}) for the relationships of stretch total length to body length (BL) and total rostrum length (TRL); derived age at maturity ($t_{IM,mat}$), derived length-at-maturity proportion ($\%L_\infty$); and age at which length is zero (t_0). Estimates are provided for males (M), females (F), and pooled sexes (P). The combined model was fitted to the full dataset composed of 3 sources, vertebral band counts, mark-recapture data, and results from increment analysis, and the other models were fitted to only a single data source. Band counts and increment data are for vertebrae of smalltooth sawfish collected in Florida from 2003 through 2024, and mark-recapture data are from fishery-independent surveys conducted in southwest Florida during approximately the same 20-year period.

Parameter	Sex	Model			
		Combined	Vertebral	Mark-recapture	Increment
L_∞	F	484 (466–504)	470 (418–514)	447 (389–515)	522 (492–556)
L_∞	M	446 (425–467)	429 (380–471)	420 (375–478)	490 (450–521)
L_∞	P	464 (451–481)	449 (413–479)	435 (396–480)	505 (480–528)
k	F	0.170 (0.157–0.184)	0.185 (0.140–0.223)	0.202 (0.156–0.249)	0.143 (0.127–0.159)
k	M	0.178 (0.163–0.198)	0.198 (0.151–0.246)	0.211 (0.170–0.259)	0.143 (0.125–0.161)
k	P	0.174 (0.162–0.186)	0.191 (0.159–0.222)	0.206 (0.175–0.242)	0.143 (0.129–0.155)
L_0	P	73.7 (73.3–74.1)	73.8 (72.7–75.2)	73.4 (72.0–74.6)	73.7 (73.3–74.1)
σ	P	0.0731 (0.0692–0.0770)	0.0749 (0.0631–0.0881)	0.0749 (0.0626–0.0878)	0.073 (0.0692–0.0773)
σ_{VC}	F	0.189 (0.159–0.220)	0.188 (0.159–0.216)	–	–
σ_{VC}	M	0.162 (0.131–0.190)	0.163 (0.138–0.197)	–	–
σ_{VC}	P	0.175 (0.155–0.197)	0.175 (0.154–0.197)	–	–
σ_{MR}	P	0.0635 (0.0541–0.0714)	–	0.0460 (0.0393–0.0553)	–
σ_{MR}	P	0.0519 (0.0462–0.0583)	–	–	0.0424 (0.0398–0.0451)
$\beta_{BL,0}$	P	1.27 (1.27–1.27)	1.27 (1.27–1.27)	–	–
$\beta_{BL,1}$	P	3.49 (3.34–3.65)	3.5 (3.35–3.67)	–	–
σ_{BL}	P	0.0146 (0.0142–0.0151)	0.0147 (0.0142–0.0151)	–	–
$\beta_{TRL,0}$	P	4.57 (4.54–4.59)	4.57 (4.54–4.59)	–	–
$\beta_{TRL,1}$	P	8.80 (–9.42 to –8.16)	–8.79 (–9.47 to –8.27)	–	–
σ_{TRL}	P	0.0526 (0.051–0.0541)	0.0526 (0.0512–0.0541)	–	–
$t_{IM,mat}$	F	7.6 (7.13–7.94)	7.5 (6.52–8.48)	7.8 (6.39–9.67)	7.6 (6.99–8.11)
$t_{IM,mat}$	M	7.1 (6.64–7.52)	7.1 (6.02–8.03)	6.9 (5.87–8.11)	7.2 (6.55–7.69)
$t_{IM,mat}$	P	7.3 (7.03–7.65)	7.3 (6.67–8.00)	7.4 (6.51–8.45)	7.4 (6.90–7.77)
$\%L_\infty$	F	0.765 (0.734–0.794)	0.787 (0.710–0.874)	0.827 (0.699–0.927)	0.709 (0.665–0.751)
$\%L_\infty$	M	0.763 (0.727–0.800)	0.792 (0.703–0.871)	0.810 (0.705–0.899)	0.695 (0.641–0.741)
$\%L_\infty$	P	0.765 (0.739–0.788)	0.791 (0.734–0.851)	0.817 (0.739–0.896)	0.702 (0.670–0.737)
t_0	F	–0.972 (–1.020 to –0.921)	–0.923 (–1.060 to –0.794)	–0.888 (–0.971 to –0.785)	–1.06 (–1.14 to –0.99)
t_0	M	–1.020 (–1.070 to –0.952)	–0.953 (–1.100 to –0.823)	–0.909 (–1.010 to –0.810)	–1.14 (–1.23 to –1.04)
t_0	P	–0.994 (–1.040 to –0.950)	–0.937 (–1.040 to –0.839)	–0.898 (–0.968 to –0.833)	–1.10 (–1.17 to –1.04)

mature male was 6.8 years (no length was recorded for this individual because its caudal fin was missing). For females, the resulting age at 50% maturity was estimated at 7.9 years (95% CI: 6.9–8.8 years). The oldest immature female was 7.9 years (365 cm STL), and the youngest mature female was 7.0 years (413 cm STL).

Natural mortality

Using the natural mortality surrogates, the known maximum age in our dataset, and the VBGF parameters, we estimated median constant mortality rates of 0.151–0.278 (Fig. 6A). The Then et al. (2015) VBGF estimator, the use

of which resulted in a natural mortality rate of 0.151, was the most certain, followed by the Pauly (1980) and Jensen (1996) estimators with estimated rates of 0.240 and 0.278. The estimators of maximum observed age from Hoenig (1983) and Then et al. (2015), with which we estimated natural mortality rates of 0.179 and 0.217, had no associated uncertainty. Natural mortality at age was highest for young individuals (<2.5 years old) when the Lorenzen et al. (2022) estimator was used and lowest when the Peterson and Wroblewski (1984) estimator was used (Fig. 6B). At the maximum observed age (30.1 years), estimates of natural mortality produced with all estimators are similar, but the estimate made with the Chen and Watanabe

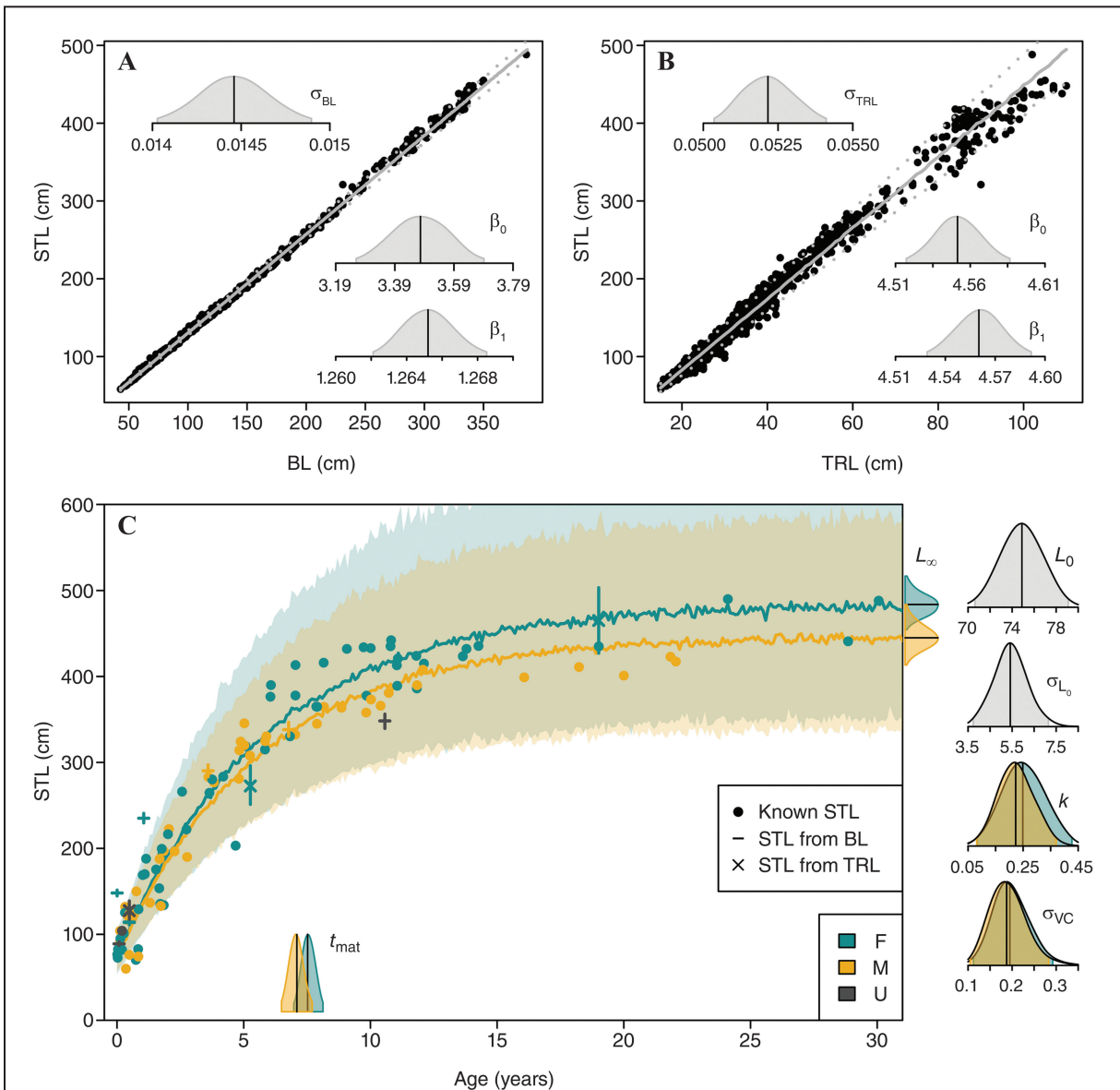
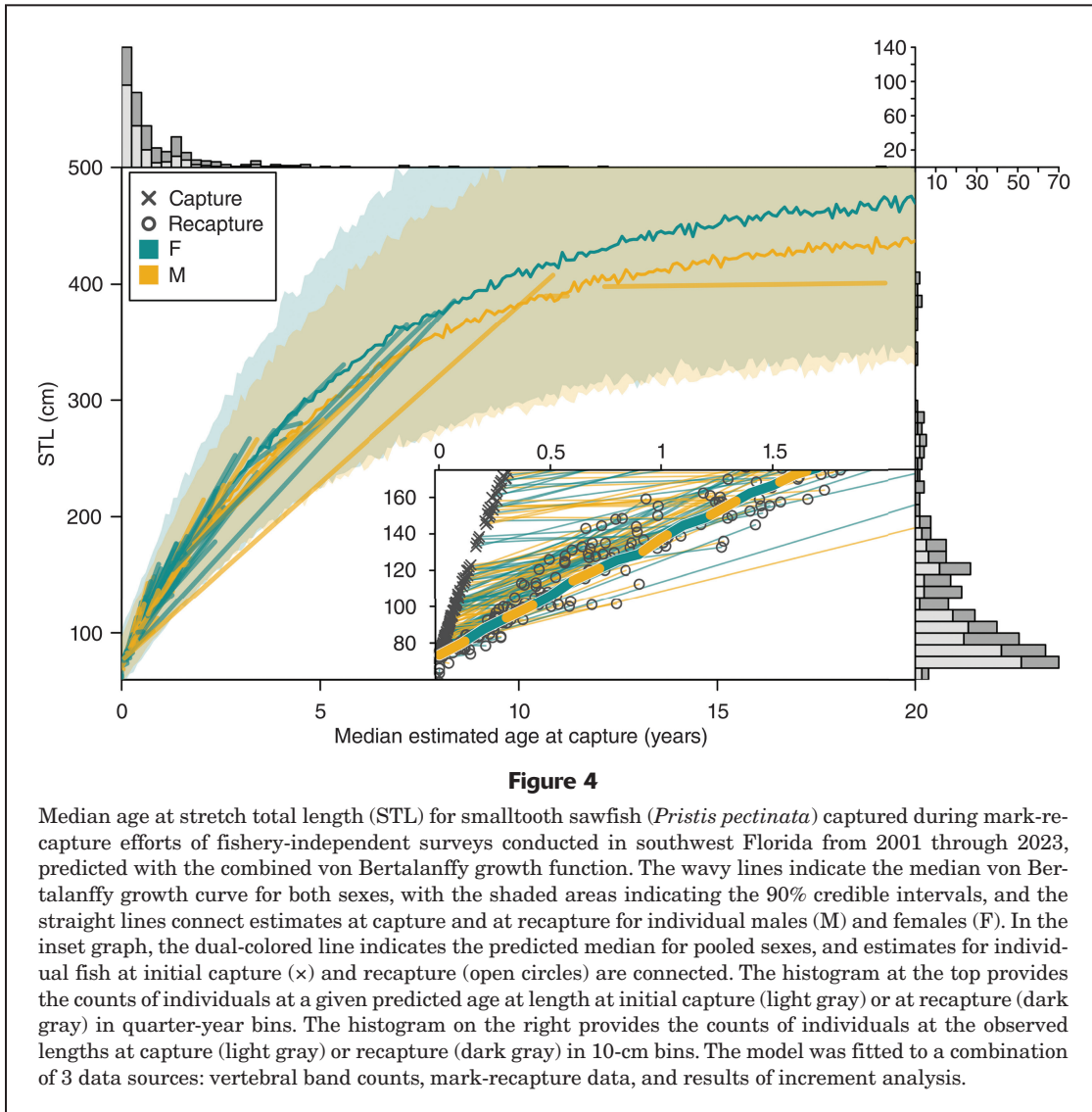


Figure 3

Relationships of stretch total length (STL) to (A) body length (BL) and (B) total rostral length (TRL) for smalltooth sawfish (*Pristis pectinata*), based on data from fishery-independent surveys conducted in southwest Florida from 2001 through 2023. In panels A and B, solid lines indicate the median prediction, dotted lines indicate the 90% credible interval, and the insets show the posterior distributions of the intercept (β_0), slope (β_1), and standard deviation (σ). (C) Lengths at age for males (M), females (F), and individuals of unknown sex (U) are shown as follows: dots indicate known STLs, vertical segments indicate estimated STLs (on these segments, horizontal bars indicate the STL-BL relationship used and crossed bars indicate the STL-TRL relationship used), solid lines indicate the median von Bertalanffy growth curves, and shaded areas indicate the 90% credible intervals. Also shown are the posterior distributions of asymptotic length (L_∞), length at birth (L_0), variation in length at birth (σ_{L_0}), Brody growth coefficient (k), variation in growth (σ_{VC}), and age at maturity (t_{mat}). In each posterior distribution graph, the vertical bar is the median and the shaded area is the 90% credible interval. The growth model was fitted to a combination of 3 data sources: vertebral band counts, mark-recapture data, and results from increment analysis. Band counts and increment data are for vertebrae collected in Florida from 2003 through 2024, and mark-recapture data are from fishery-independent surveys.

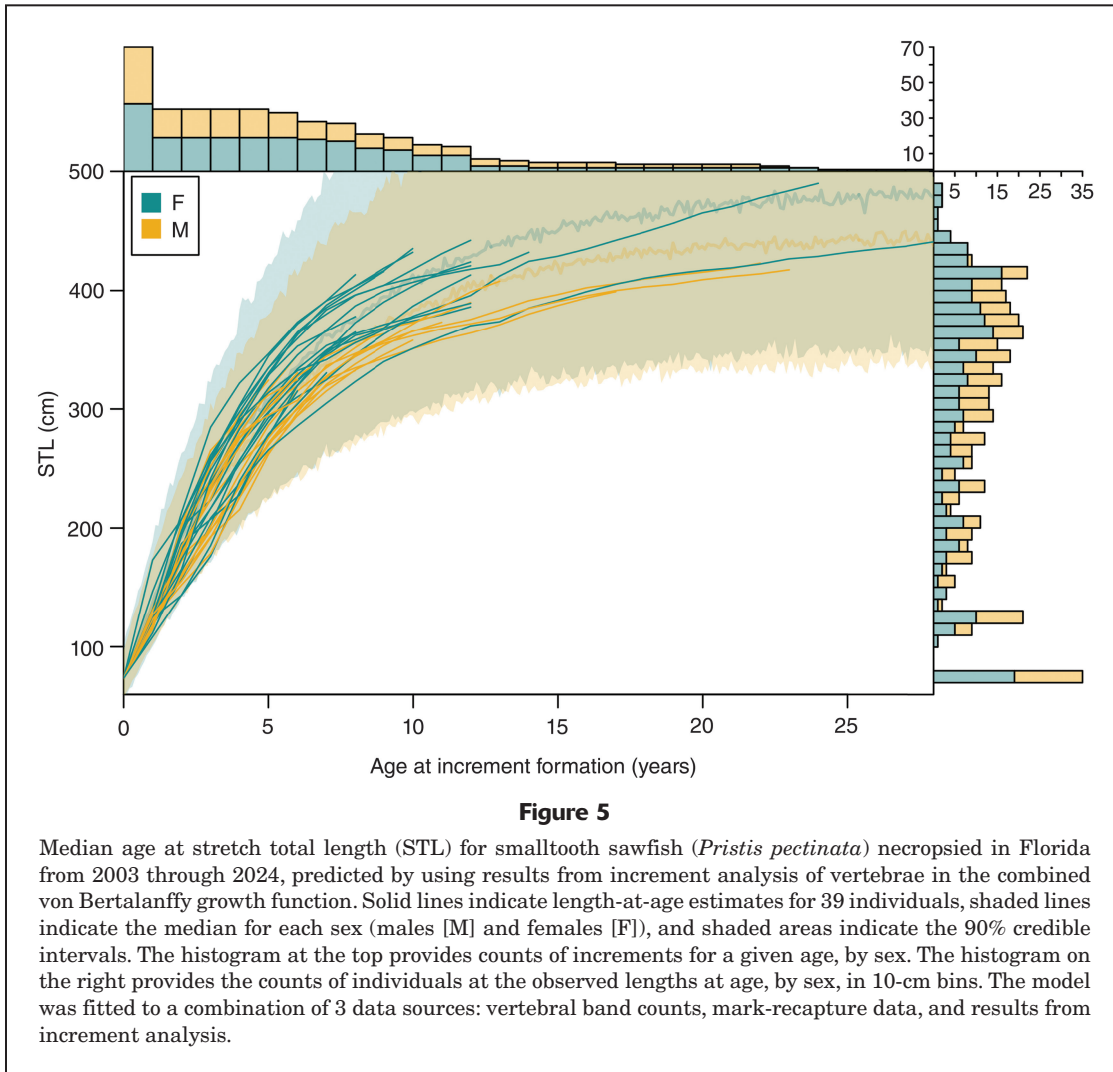


(1989) estimator is the lowest and the rate estimated with the Lorenzen (1996) estimator is the highest. The estimate of natural mortality when the population reaches its L_{∞} , calculated with the Lorenzen et al. (2022) estimator, is 0.200 (90% credible interval: 0.185–0.216), a level between those produced with the Hoenig (1983) estimator and the Then et al. (2015) estimator of maximum observed age. This analysis resulted in a ratio of natural mortality to k of 1.15 (90% credible interval: 1.14–1.16).

Discussion

In this study, we improved knowledge of the life history of the smalltooth sawfish by estimating somatic growth across 3 datasets, accounting for various sources of uncertainty, and deriving critical estimates of length and age at maturity, constant natural mortality, and natural mortality at age. Previous estimates of growth were constrained by small sample sizes, single sources of

length-at-age data, and bias from an overrepresentation of juveniles. The approach we took to the combination of traditional vertebral-band-count, mark-recapture, and increment back-calculation datasets represents a novel framework for integrating multiple sources of growth information. Additionally, the results of this study indicate that data from carcasses can be used for length-length relationships jointly estimated within the model and that the associated uncertainty in those estimated relationships can be included in the VBGF estimation. The derived age-at-maturity estimates are not significantly different from direct estimates, providing the first support for the use of life history surrogates for a sawfish species. Together, the estimates of somatic growth, length and age at maturity, and natural mortality can be used to refine population growth and viability models. Given the endangered status of the smalltooth sawfish, improving the inputs to these risk and recovery models will result in more effective management and conservation strategies.



Age and growth

The oldest smalltooth sawfish in this study was a 30.1-year-old female measuring 488.2 cm STL, and the oldest male was 22.1 years old and 417.4 cm STL. These ages surpass those reported by Scharer et al. (2012), with the oldest individual in that study a 435-cm-STL female estimated to be 14 years old. By using the growth model of Scharer et al. (2012), the maximum age in the wild has been estimated to be 30 years (Carlson and Simpfordorfer, 2015), which we now know is attainable. For comparison, the oldest known captive smalltooth sawfish was a male held in the United States from 1 June 1968 to 8 January 2012, for a life of over 43 years (White and Henningsen²). The longest-held smalltooth sawfish that is still living is a male that has been kept at SeaWorld Orlando since

November 1989 (White and Henningsen²). For the large-tooth sawfish (*P. pristis*), the maximum observed age is 44 years in the Indo-West Pacific, slightly longer than the estimated longevity of 41 years for that species (Tanaka, 1991). Therefore, it is likely that smalltooth sawfish can live longer than what we observed in this study.

In comparison to those of previous research, our study benefited from a larger sample size, providing more robust growth estimates that indicate that growth of smalltooth sawfish is marginally slower than previously reported. The *k* for both sexes in our study was 0.174 year⁻¹, lower than the 0.22 year⁻¹ reported by Scharer et al. (2012). The smalltooth sawfish grows faster than its congeners, the largetooth sawfish in the western Atlantic Ocean (0.05–0.07 year⁻¹; Kyne et al., 2021) and the green sawfish (*P. zijsron*) in the eastern Indian Ocean (0.090 year⁻¹; Lear et al., 2023). We predicted length at age 1 to be 136 cm STL (for pooled sexes), smaller than the 147 cm STL reported by Scharer et al. (2012) and likely more reliable given our larger sample size. Our study included vertebrae from fish with a broad range of lengths, from a 60-cm-STL male to

² White, S., and A. Henningsen. 2017. North American regional studbook for Pristidae species, 23 p. Ripley Entertainment, Myrtle Beach, SC. [Available from Ripley’s Aquarium of Myrtle Beach, 1110 Celebrity Cir., Myrtle Beach, SC 29577.]

a 490-cm-STL female. The longest sawfish in our study is the largest smalltooth sawfish to have been reliably measured in recent decades, and its length aligns with the expected maximum noted in Brame et al. (2019), although it is smaller than the historically known maximum of at least 553 cm STL (Bigelow and Schroeder, 1953). Smith et al. (2024) also noted that both existing records and

historical specimens indicate that this species likely once reached greater lengths but over time has experienced a reduction in maximum length, a pattern reported for over-exploited fish populations (e.g., Longhurst, 2002; Charbonneau et al., 2019).

Estimated ages vary considerably among individuals of the same length, even though vertebrae were taken consistently from below the first dorsal fin. For example, the ages estimated from vertebral band counts for 3 females measuring 435 cm STL range from 10.8 to 19.0 years. This age variability is not unexpected as mature size classes typically have more age variability than immature size classes. After reaching maturity, somatic growth is influenced by the energy allocated to reproduction (e.g., to growth and development of reproductive tissues, egg or sperm production, mating, and associated migrations; Brown et al., 2004; Brunel et al., 2013; Wilson et al., 2018). Additional variability can be explained by the increase in weight. For example, in the 400–440-cm length class in our study, weights of necropsied specimens ranged from 172.5 to 270.2 kg for males and from 192.7 to 251.2 kg for females. Other factors, such as environmental conditions, prey availability, genetics, and overall health, could contribute to this variability.

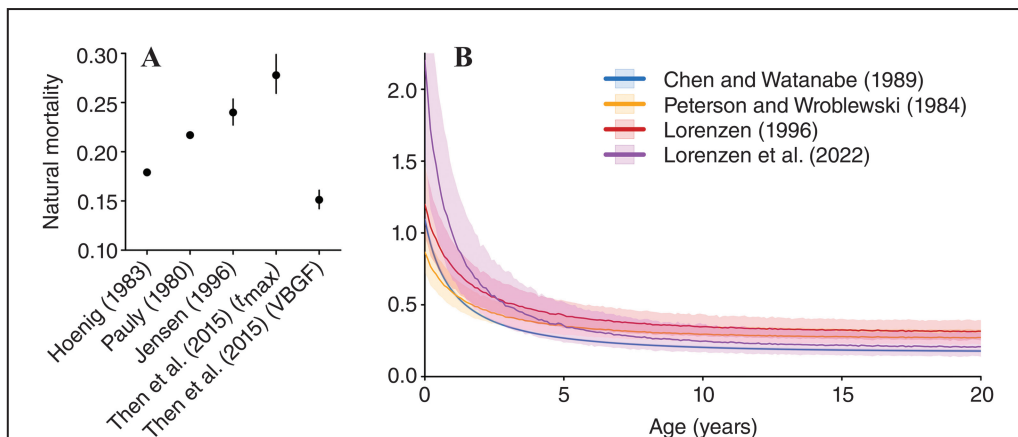
Maturity

Understanding maturity is crucial for assessing the reproductive potential of a species and its ability to recover from population decline and, thereby, for guiding conservation efforts and ensuring long-term species viability. Prior to this study, there was considerable uncertainty regarding age and length at maturity due to the limited number of necropsied adults. On the basis of VBGF estimates from Scharer et al. (2012), Carlson and Simpfendorfer (2015) suggested that maturity occurs between 7 and 11 years for

Table 4

Probability of the maximum a posteriori estimates of the difference between sex-specific parameter estimates being equal to zero for estimation in each of the 4 von Bertalanffy growth functions used to examine age and growth of smalltooth sawfish (*Pristis pectinata*). The parameters are asymptotic length (L_{∞}), Brody growth coefficient (k), variability in length at age based on vertebral band counts (σ_{VC}), and derived age at maturity ($t_{IM, mat}$). An asterisk (*) indicates the parameter for which there was a significant difference ($P < 0.1$). The combined model was fitted to the full dataset composed of 3 sources, vertebral band counts, mark-recapture data, and results from increment analysis, and the other models were fitted to only a single data source. Band counts and increment data are for vertebrae of smalltooth sawfish collected in Florida from 2003 through 2024, and mark-recapture data are from fishery-independent surveys conducted in southwest Florida during approximately the same 20-year period.

Parameter	Combined	Vertebral	Mark-recapture	Increment
L_{∞}	0.07*	0.63	0.77	0.50
k	0.76	0.92	0.95	1
σ_{VC}	0.59	0.54	–	–
$t_{IM, mat}$	0.42	0.89	0.76	0.59



Median estimates of (A) constant natural mortality (points) and (B) mortality at age (solid lines) for smalltooth sawfish (*Pristis pectinata*), predicted by using estimators based on maximum observed age (t_{max}) and posterior distributions of parameters of the von Bertalanffy growth function (VBGF) (for more information about these surrogate estimators, see Table 2). Error bars in panel A and shaded areas in panel B indicate 90% credible intervals.

both sexes, with Carlson (2023) estimating median age of maturity for females at 8 years. An unprecedented mortality event in the Florida Keys during early 2024 led to the death of at least 56 large smalltooth sawfish (>314.2 cm STL), from which we obtained vertebral centra from 38 individuals. This event, along with previously necropsied individuals, increased our sample size, enhancing the precision of our maturity estimates with data from 34 mature (19 females and 15 males) and 72 immature (40 females and 32 males) individuals of known sex.

Although our revised estimates are similar to those from previous studies, they offer greater precision because of larger sample sizes and because of the use of observed developmental state of reproductive organs for both sexes. The length-at-maturity estimates we used in the VBGF back-calculation and reported by Brame et al. (2019) were based on testosterone levels and clasper calcification for males and estradiol levels for females. Our direct estimates of length at maturity based on the observed developmental state of reproductive organs are slightly higher for males (by 5 cm STL) and females (by 13 cm STL). However, the largest immature male was 346 cm STL, and the smallest mature male was 345 cm STL, sizes closely aligned with the estimates of Brame et al. (2019). Direct estimates of age at maturity differ slightly from those from the VBGF, with males reaching 50% maturity at a slightly younger age (6.9 years) and females reaching maturity at a slightly older age (7.9 years). Both direct estimates are within the 90% credible intervals for age at maturity, back-calculated by using the lengths at maturity from Brame et al. (2019) in the VBGF, indicating that there are no significant differences in estimates between the direct and indirect methods. These results also support the use of 76.5% of L_{∞} as a surrogate estimation of length at maturity for smalltooth sawfish and, perhaps, for other sawfish species.

Natural mortality

The derived estimates of constant natural mortality indicate that from 75.7% to 86.0% of smalltooth sawfish survive annually. The estimate from the use of the more reliable Then et al. (2015) VBGF estimator was at the low range among the set of estimations (0.151). This result indicates that, based on its somatic growth, the smalltooth sawfish is likely to have a lower natural mortality than would be expected from estimations with most common natural mortality surrogates, which have been used in past population viability analyses (Carlson and Simpendorfer, 2015; Carlson, 2023). When estimators from Then et al. (2015) were used, the survival estimate from the VBGF estimator was higher than the estimate from the maximum observed age, indicating that the true maximum age is older than 30.1 years, the maximum age in our study. Given the current low population size of the species, this result is unsurprising. Use of the maximum age that would produce the Then et al. (2015) VBGF estimate of natural mortality resulted in a hypothetical maximum age of 44.6 years. Although hypothetical, this age estimate

provides some idea about the erosion of the age structure of smalltooth sawfish in Florida due to anthropogenic effects.

We provide updated estimates of natural mortality at age from the use of several historical surrogate equations, but the estimator of Lorenzen et al. (2022) was the most robust and should be used. Therefore, it draws into question the population viability analysis by Carlson (2023), who employed several surrogates to estimate natural mortality at age, including Lorenzen (1996), but did not use the updated estimator from Lorenzen et al. (2022) in his projections. Predictions of natural mortality from the Lorenzen et al. (2022) surrogate equation are higher for individuals less than 2.5 years old and lower for individuals greater than 2.5 years old than estimates from the Lorenzen (1996) surrogate estimator. Therefore, the differential effects on smalltooth sawfish that result from their ontogeny will confer different effects to the overall population and its recovery potential. For example, recent concerns about bycatch in the shrimp-trawl fishery and unprecedented mortality events in the Florida Keys and Florida Bay have raised concerns about adult mortality (e.g., Graham et al., 2022). If adults continue to experience elevated mortality from bycatch and extreme mortality events, combined with high natural mortality in the first 2.5 years, extinction risk would certainly increase.

Given the slow growth and delayed maturity of sawfishes, ensuring the stability of adult populations is crucial for their long-term viability. The distinction between Type I (high age at maturity, low natural mortality, and slow growth with larger L_{∞}) and Type II (earlier sexual maturity, higher natural mortality, and faster growth with lower L_{∞}) chondrichthyans (Prince et al., 2015) influences mortality-at-age relationships used in population models and is important to identify. According to results from use of the most recently published estimator, the method used by Lorenzen et al. (2022), the smalltooth sawfish would be classified as a Type I chondrichthyan, with a ratio of natural mortality to k of 1.15 at L_{∞} (Prince et al., 2015). However, the median estimates of natural mortality from the Then et al. (2015) VBGF mean that the ratio of natural mortality to k is >1, indicating ambiguity regarding the classification of this species as Type I. This ambiguity is extended by our estimated proportion of L_{∞} being more similar to the 75% of L_{∞} that is typical for Type II chondrichthyans than the 55% of L_{∞} that is typical for Type I chondrichthyans (Prince et al., 2015). This uncertainty may arise from underestimation of natural mortality or the omission of sawfishes in life history invariant estimates. Ultimately, the smalltooth sawfish has characteristics of the Type I and Type II classifications: high longevity, moderate age at maturity, slow growth, and moderate natural mortality.

Challenges in age estimation

Age estimation for smalltooth sawfish, particularly older individuals, can present a challenge because of the nature of vertebral band formation. In younger individuals (<6

years), growth band formation in the vertebrae was generally consistent and clear, making age interpretation straightforward. As individuals grew larger, the outer bands became more tightly spaced and stacked, a common phenomenon observed in other elasmobranchs (Cailliet and Goldman, 2004), but they remained distinguishable. Growth band deposition is closely linked to somatic growth in several elasmobranchs (Natanson et al., 2018). Some species, such as the porbeagle (*Lamna nasus*) and sandbar shark (*Carcharhinus plumbeus*), experience a slowing or cessation of band deposition at older ages (>25 years) (Francis et al., 2007; Andrews et al., 2011). Although inconsistencies in band-pair formation may lead to age underestimation, as has been observed for various elasmobranch species (Francis et al., 2007; Andrews et al., 2011; Harry et al., 2013; Passerotti et al., 2014; Natanson et al., 2018; James and Natanson, 2021), they have not been documented for sawfishes.

Conclusions

Challenges faced by the smalltooth sawfish, particularly the threat of large individuals becoming bycatch in the shrimp-trawl fishery and their recent elevated mortality rates, demand focused conservation efforts to mitigate these risks and support population stability. With a better understanding of the life history of this species and the effects of changing mortality dynamics, conservation strategies can be refined to protect smalltooth sawfish and ensure their long-term survival. The results of our study underscore the importance of continued monitoring and data collection to inform and support long-term recovery efforts. Furthermore, our study, along with previous research, highlights the need for tailored strategies, including habitat protection in known areas of high use by juveniles (see Scharer et al., 2017) and stricter fishing regulations (e.g., closure areas for shrimp trawling; see figure 8 in Graham et al., 2022), to reduce mortality and protect critical habitats. Managing these mortality risks is vital to maintaining a balanced age structure and to supporting population recovery.

Resumen

Las estimaciones precisas de la edad, el crecimiento somático, la madurez y la mortalidad natural son esenciales para la conservación eficaz de las especies amenazadas. Este estudio actualiza datos sobre el crecimiento y las primeras evaluaciones directas de la longitud de madurez y la edad de madurez de la especie amenazada de pez sierra (*Pristis pectinata*). Se realizó una estimación Bayesiana utilizando la función de crecimiento de von Bertalanffy para combinar los conteos de bandas vertebrales, los datos de marcado-recaptura y los resultados del análisis de incrementos para estimar el crecimiento somático y determinar la edad de madurez y las tasas de mortalidad natural. El pez sierra crece rápidamente en sus primeros 3 años,

alcanzando 235 cm de longitud total estirada (STL), 3.2 veces su longitud promedio al nacer (73.7 cm STL), antes de que el crecimiento desacelere. La longitud asintótica fue de 446 cm STL para los machos y 484 cm STL para las hembras, con un coeficiente de crecimiento de 0.178 año⁻¹ para los machos y 0.170 año⁻¹ para las hembras. Estimamos directamente la edad mediana de madurez en 6.9 años para los machos y 7.9 años para las hembras, similar a evaluaciones indirectas previas. La mortalidad natural constante se estimó entre 0.151 y 0.278 a partir de sustitutos del ciclo de vida. El individuo más viejo examinado en este estudio fue una hembra de 30.1 años, lo que confirma que la especie supera los 30 años en estado silvestre. Estos resultados son vitales para perfeccionar los modelos de recuperación de la población y subrayan la necesidad de un seguimiento continuo y la colecta de datos para apoyar los esfuerzos de recuperación a largo plazo.

Acknowledgments

We thank T. Wiley and D. Grubbs, members of the Smalltooth Sawfish Recovery Implementation Team, for contributing survey data to construct length relationships; K. Feldheim for providing genetic data to assign birth dates; E. Fortman for assistance with producing Figure 2, and A. Hilton for assisting with processing vertebrae. We thank A. Brame, B. Moe, and 3 anonymous reviewers for comments and insights that improved the manuscript. This research was funded primarily by the National Marine Fisheries Service under Section 6 (Cooperation with the States) of the U.S. Endangered Species Act through multiple grant awards to the Florida Fish and Wildlife Conservation Commission (NA06NMF4720032, NA10NMF4720032, NA13NMF4720047, NA16NMF4720062, NA19NMF4720108, and NA22NMF4720102). Research was conducted by the senior author, in part, under the auspices of the Cooperative Institute for Marine and Atmospheric Studies, which is based at the University of Miami and funded by NOAA (cooperative agreement NA20OAR4320472).

Literature cited

- Andrews, A. H., L. J. Natanson, L. A. Kerr, G. H. Burgess, and G. M. Cailliet.
2011. Bomb radiocarbon and tag-recapture dating of sandbar shark (*Carcharhinus plumbeus*). *Fish. Bull.* 109:454–465.
- Beamish, R. J., and D. A. Fournier.
1981. A method for comparing the precision of a set of age determinations. *Can. J. Fish. Aquat. Sci.* 38:982–983. [Crossref](#)
- Beissinger, S. R., and D. R. McCullough (eds.).
2002. Population viability analysis, 593 p. Univ. Chicago Press, Chicago, IL.
- Bigelow, H. B., and W. C. Schroeder.
1953. Fishes of the western North Atlantic. Part 2: sawfishes, guitarfishes, skates and rays, chimaeroids, 588 p. Sears Found. Mar. Res., Yale Univ., New Haven, CT.

- Brame, A. B., T. R. Wiley, J. K. Carlson, S. V. Fordham, R. D. Grubbs, J. Osborne, R. M. Scharer, D. M. Bethea, and G. R. Poulakis. 2019. Biology, ecology, and status of the smalltooth sawfish *Pristis pectinata* in the USA. *Endanger. Species Res.* 39:9–23. [Crossref](#)
- Brown, J. H., J. F. Gillooly, A. P. Allen, V. M. Savage, and G. B. West. 2004. Toward a metabolic theory of ecology. *Ecology* 85:1771–1789. [Crossref](#)
- Brunel, T., B. Ernande, F. M. Mollet, and A. D. Rijnsdorp. 2013. Estimating age at maturation and energy-based life-history traits from individual growth trajectories with nonlinear mixed-effects models. *Oecologia* 172:631–643. [Crossref](#)
- Cailliet, G. M., and K. J. Goldman. 2004. Age determination and validation in chondrichthyan fishes. In *Biology of sharks and their relatives* (J. C. Carrier, J. A. Musick, and M. R. Heithaus, eds.), p. 399–447, CRC Press, Boca Raton, FL.
- Caltabellotta, F. P., Z. A. Siders, D. J. Murie, F. S. Motta, G. M. Cailliet, and O. B. F. Gadig. 2019. Age and growth of three endemic threatened guitarfishes *Pseudobatos horkelii*, *P. percellens* and *Zapteryx brevirostris* in the western South Atlantic Ocean. *J. Fish Biol.* 95:1236–1248. [Crossref](#)
- Caltabellotta, F. P., Z. A. Siders, G. M. Cailliet, F. S. Motta, and O. B. F. Gadig. 2021. Preliminary age and growth of the deep-water goblin shark *Mitsukurina owstoni* (Jordan, 1898). *Mar. Freshw. Res.* 72:432–438. [Crossref](#)
- Carlson, J. K. 2023. Trouble in the trawls: is bycatch in trawl fisheries preventing the recovery of sawfish? A case study using the US population of smalltooth sawfish, *Pristis pectinata*. *Global Ecol. Conserv.* 48:e02745. [Crossref](#)
- Carlson, J. K., and C. A. Simpfendorfer. 2015. Recovery potential of smalltooth sawfish, *Pristis pectinata*, in the United States determined using population viability models. *Aquat. Conserv.* 25:187–200. [Crossref](#)
- Chamberlin, D. W., Z. A. Siders, B. K. Barnett, and W. F. Patterson III. 2023. Eye lens-derived $\Delta^{14}\text{C}$ signatures validate extreme longevity in the deepwater scorpaenid blackbelly rosefish (*Helicolenus dactylopterus*). *Sci. Rep.* 13:7438. [Crossref](#)
- Chamberlin, D. W., Z. A. Siders, J. C. Potts, W. D. Rogers, M. A. Taylor, and W. F. Patterson III. 2025. Bayesian estimation of von Bertalanffy growth parameters for gray triggerfish, *Balistes caprisacus*, incorporating multiple readers and ageing structures. *Can. J. Fish. Aquat. Sci.* [Crossref](#)
- Charbonneau, J. A., D. M. Keith, and J. A. Hutchings. 2019. Trends in the size and age structure of marine fishes. *ICES J. Mar. Sci.* 76:938–945. [Crossref](#)
- Chen, S., and S. Watanabe. 1989. Age dependence of natural mortality coefficient in fish population dynamics. *Nippon Suisan Gakkaishi* 55:205–208. [Crossref](#)
- Dulvy, N. K., L. N. K. Davidson, P. M. Kyne, C. A. Simpfendorfer, L. R. Harrison, J. K. Carlson, and S. V. Fordham. 2016. Ghosts of the coast: global extinction risk and conservation of sawfishes. *Aquat. Conserv.* 26:134–153. [Crossref](#)
- Fabens, A. J. 1965. Properties and fitting of the von Bertalanffy growth curve. *Growth* 29:265–289.
- Federal Register. 2003. Endangered and threatened species; final endangered status for a distinct population segment of smalltooth sawfish (*Pristis pectinata*) in the United States. Fed. Reg. 68:15674–15680. [Available from [website](#).]
- Francis, M. P., S. E. Campana, and C. M. Jones. 2007. Age under-estimation in New Zealand porbeagle sharks (*Lamna nasus*): is there an upper limit to ages that can be determined from shark vertebrae? *Mar. Freshw. Res.* 58:10–23. [Crossref](#)
- Gabry, J., R. Češnovar, A. Johnson, and S. Bröder. 2024. cmdstanr: R interface to ‘CmdStan.’ R package, vers. 0.8.1. [Available from [website](#), accessed March 2025.]
- Gelman, A., and D. B. Rubin. 1992. Inference from iterative simulation using multiple sequences. *Stat. Sci.* 7:457–472. [Crossref](#)
- Graham, J., A. M. Kroetz, G. R. Poulakis, R. M. Scharer, J. K. Carlson, S. K. Lowerre-Barbieri, D. Morley, E. A. Reyier, and R. D. Grubbs. 2022. Commercial fishery bycatch risk for large juvenile and adult smalltooth sawfish (*Pristis pectinata*) in Florida waters. *Aquat. Conserv.* 32:401–416. [Crossref](#)
- Hamlett, W. C. (ed.). 2005. Reproductive biology and phylogeny of chondrichthyes: sharks, batoids, and chimaeras, vol. 3, 572 p. Science Publishers Inc., Enfield, NH.
- Harry, A. V., A. J. Tobin, and C. A. Simpfendorfer. 2013. Age, growth and reproductive biology of the spot-tail shark, *Carcharhinus sorrah*, and the Australian blacktip shark, *C. tilstoni*, from the Great Barrier Reef World Heritage Area, north-eastern Australia. *Mar. Freshw. Res.* 64:277–293. [Crossref](#)
- Harry, A. V., J. K. Carlson, M. Espinoza, M. I. Grant, A. B. Haque, R. W. Jabado, and C. L. Rigby. 2024. All sawfish now Critically Endangered but sustained conservation efforts can lead to recovery. *Oryx* 58:146. [Crossref](#)
- Heupel, M. R., and C. A. Simpfendorfer. 2010. Science or slaughter: need for lethal sampling of sharks. *Conserv. Biol.* 24:1212–1218. [Crossref](#)
- Hoenig, J. M. 1983. Estimating total mortality rate from longevity data (fish, mollusks, cetaceans). Ph.D. diss., 92 p. Univ. Rhode Island, Kingston, RI. [Available from [website](#).]
- James, K. C., and L. J. Natanson. 2021. Positional and ontogenetic variation in vertebral centra morphology in five batoid species. *Mar. Freshw. Res.* 72:887–898. [Crossref](#)
- Jensen, A. L. 1996. Beverton and Holt life history invariants result from optimal trade-off of reproduction and survival. *Can. J. Fish. Aquat. Sci.* 53:820–822. [Crossref](#)
- Kyne, P. M., M. Oetinger, M. I. Grant, and P. Feutry. 2021. Life history of the Critically Endangered largetooth sawfish: a compilation of data for population assessment and demographic modelling. *Endanger. Species Res.* 44:79–88. [Crossref](#)
- Lear, K. O., T. Fazeldean, R. L. Bateman, J. Inglebrecht, and D. L. Morgan. 2023. Growth and morphology of Critically Endangered green sawfish *Pristis zijsron* in globally important nursery habitats. *Mar. Biol.* 170:70. [Crossref](#)
- Longhurst, A. 2002. Murphy’s law revisited: longevity as a factor in recruitment to fish populations. *Fish. Res.* 56:125–131. [Crossref](#)
- Lorenzen, K. 1996. The relationship between body weight and natural mortality in juvenile and adult fish: a comparison of natural ecosystems and aquaculture. *J. Fish Biol.* 49:627–642. [Crossref](#)

- Lorenzen, K., E. V. Camp, and T. M. Garlock.
2022. Natural mortality and body size in fish populations. *Fish. Res.* 252:106327. [Crossref](#)
- Makowski, D., M. Ben-Shachar, and D. Lüdtke.
2019. bayestestR: describing effects and their uncertainty, existence and significance within the Bayesian framework. *J. Open Source Softw.* 4(40):1541. [Crossref](#)
- Natanson, L. J., G. B. Skomal, S. L. Hoffmann, M. E. Porter, K. J. Goldman, and D. Serra.
2018. Age and growth of sharks: do vertebral band pairs record age? *Mar. Freshw. Res.* 69:1440–1452. [Crossref](#)
- Passerotti, M. S., A. H. Andrews, J. K. Carlson, S. P. Wintner, K. J. Goldman, and L. J. Natanson.
2014. Maximum age and missing time in the vertebrae of sand tiger shark (*Carcharias taurus*): validated lifespan from bomb radiocarbon dating in the western North Atlantic and southwestern Indian Oceans. *Mar. Freshw. Res.* 65:674–687. [Crossref](#)
- Pauly, D.
1980. On the interrelationships between natural mortality, growth parameters, and mean environmental temperature in 175 fish stocks. *ICES J. Mar. Sci.* 39:175–192. [Crossref](#)
- Peterson, I., and J. S. Wroblewski.
1984. Mortality rate of fishes in the pelagic ecosystem. *Can. J. Fish. Aquat. Sci.* 41:1117–1120. [Crossref](#)
- Prince, J., A. Hordyk, S. R. Valencia, N. Loneragan, and K. Sainsbury.
2015. Revisiting the concept of Beverton–Holt life-history invariants with the aim of informing data-poor fisheries assessment. *ICES J. Mar. Sci.* 72:194–203. [Crossref](#)
- Poulakis, G. R., P. W. Stevens, A. A. Timmers, T. R. Wiley, and C. A. Simpfendorfer.
2011. Abiotic affinities and spatiotemporal distribution of the endangered smalltooth sawfish, *Pristis pectinata*, in a south-western Florida nursery. *Mar. Freshw. Res.* 62:1165–1177. [Crossref](#)
- Poulakis, G. R., J. T. Wyffels, P. E. Fortman, A. K. Wooley, L. B. Heath, D. M. Yakich, and P. W. Wilson.
2024. Morphology, composition, and deterioration of the embryonic rostral sheath of the smalltooth sawfish (*Pristis pectinata*). *Fish. Bull.* 122:76–88. [Crossref](#)
- R Core Team.
2024. R: a language and environment for statistical computing. R Foundation for Statistical Computing, Vienna, Austria. [Available from [website](#), accessed July 2024.]
- Rolim, F. A., Z. A. Siders, F. P. Caltabellotta, M. M. Rotundo, and T. Vaske-Júnior.
2020. Growth and derived life-history characteristics of the Brazilian electric ray *Narcine brasiliensis*. *J. Fish Biol.* 97:396–408. [Crossref](#)
- Scharer, R. M., W. F. Patterson III, J. K. Carlson, and G. R. Poulakis.
2012. Age and growth of endangered smalltooth sawfish (*Pristis pectinata*) verified with LA-ICP-MS analysis of vertebrae. *PLoS ONE* 7(10):e47850. [Crossref](#)
- Scharer, R. M., P. W. Stevens, C. P. Shea, and G. R. Poulakis.
2017. All nurseries are not created equal: large-scale habitat use patterns in two smalltooth sawfish nurseries. *Endanger. Species Res.* 34:473–492. [Crossref](#)
- Schneider, C. A., W. S. Rasband, and K. W. Eliceiri.
2012. NIH Image to ImageJ: 25 years of image analysis. *Nat. Methods* 9:671–675 [Crossref](#)
- Siders, Z. A., T. A. Stratmann, C. N. Turner Tomaszewicz, A. D. Walde, and E. C. Munscher.
2023. Somatic growth and maturity for four species of river cooter including *Pseudemys concinna suwanniensis*, *P. nelsoni*, *P. peninsularis*, and *P. texana*. *Biology* 12(7):965. [Crossref](#)
- Simpfendorfer, C. A.
2000. Predicting population recovery rates for endangered western Atlantic sawfishes using demographic analysis. *Environ. Biol. Fishes* 58:371–377. [Crossref](#)
- Simpfendorfer, C. A., G. R. Poulakis, P. M. O'Donnell, and T. R. Wiley.
2008. Growth rates of juvenile smalltooth sawfish *Pristis pectinata* Latham in the western Atlantic. *J. Fish Biol.* 72:711–723. [Crossref](#)
- Smart, J. J., A. V. Harry, A. J. Tobin, and C. A. Simpfendorfer.
2013. Overcoming the constraints of low sample sizes to produce age and growth data for rare or threatened sharks. *Aquat. Conserv.* 23:124–134. [Crossref](#)
- Smith, K. L., A. Fearing, N. M. Phillips, A. M. Kroetz, T. R. Wiley, J. K. Carlson, and S. S. Taylor.
2024. Historical specimens and photographs reveal long-term changes in smalltooth sawfish (*Pristis pectinata*) age class distribution and average size during U.S. population decline. *Aquat. Conserv.* 34(2):e4084. [Crossref](#)
- Stan Development Team.
2024. Stan reference manual, version 2.36, 218 p. [Available from [website](#), accessed March 2025.]
- Stehmann, M. F. W.
2002. Proposal of a maturity stages scale for oviparous and viviparous cartilaginous fishes (Pisces, Chondrichthyes). *Arch. Fish. Mar. Res.* 50:23–48.
- Suriyamongkol, T., Z. A. Siders, and I. Mali.
2024. Conservation implications of somatic growth and length-at-age in *Pseudemys gorzugi*, Rio Grande Cooter. *Hydrobiologia* 851:3525–3539. [Crossref](#)
- Tanaka, S.
1991. Age estimation of freshwater sawfish and sharks in northern Australia and Papua New Guinea. *Univ. Mus., Univ. Tokyo, Nat. Cult.* 3:71–82.
- Taylor, N. G., C. J. Walters, and S. J. D. Martell.
2005. A new likelihood for simultaneously estimating von Bertalanffy growth parameters, gear selectivity, and natural and fishing mortality. *Can. J. Fish. Aquat. Sci.* 62:215–223. [Crossref](#)
- Then, A. Y., J. M. Hoenig, N. G. Hall, and D. A. Hewitt.
2015. Evaluating the predictive performance of empirical estimators of natural mortality rate using information on over 200 fish species. *ICES J. Mar. Sci.* 72:82–92. [Crossref](#)
- von Bertalanffy, L.
1938. A quantitative theory of organic growth (inquiries on growth laws. II). *Hum. Biol.* 10:181–213.
- Wilson, K. L., A. E. Honsey, B. Moe, and P. Venturelli.
2018. Growing the biphasic framework: techniques and recommendations for fitting emerging growth models. *Methods Ecol. Evol.* 9:822–833. [Crossref](#)